Available online at www.sciencedirect.com
ScienceDirect
Journal of Bionic Engineering 14 (2017) 476–485

Biomimetic Hydrophobic Surfaces with Low or High Adhesion Based on Poly(vinyl alcohol) and SiO_2 Nanoparticles

Qian Wang[1], Zhao Dong[1], Xiaoxia Yan[1], Yanjiao Chang[1], Lili Ren[1,2], Jiang Zhou[1]

1. *Key Laboratory of Bionic Engineering* (*Ministry of Education*, *China*), *College of Biological and Agricultural Engineering*, *Jilin University*, *Changchun* 130022, *China*
2. *College of Chemistry*, *Jilin University*, *Changchun* 130022, *China*

Abstract

Superhydrophobic surfaces are often found in nature, such as plant leaves and insect wings. Inspired by superhydrophobic phenomenon of the rose petals and the lotus leaves, biomimetic hydrophobic surfaces with high or low adhesion were prepared with a facile drop-coating approach in this paper. Poly(vinyl alcohol) (PVA) was used as adhesive and SiO_2 nanoparticles were used to fabricate surface micro-structure. Stearic acid or dodecafluoroheptyl-propyl-trimethoxysilane (DFTMS) were used as low surface energy materials to modify the prepared PVA/SiO_2 coating surfaces. The effects of size of SiO_2 nanoparticles, concentration of SiO_2 nanoparticle suspensions and the modifications on the wettability of the surface were investigated. The morphology of the PVA/SiO_2 coating surfaces was observed by using scanning electron microscope. Water contact angle of the obtained superhydrophilic surface could reach to 3˚. Stearic acid modified PVA/SiO_2 coating surfaces showed hydrophobicity with high adhesion. By mixing the SiO_2 nanoparticles with sizes of 40 nm and 200 nm and modifying with DFTMS, water contact angle of the obtained coating surface could be up to 155˚ and slide angle was only 5˚. This work provides a facile and useful method to control surface wettability through changing the roughness and chemical composition of a surface.

Keywords: biomimetic surface, PVA/SiO_2 coating, hydrophobicity, high adhesion, low adhesion

doi: 10.1016/S1672-6529(16)60413-4

1 Introduction

The extreme water wetting properties of surfaces have been of great interest within the scientific community over the past decade and are gradually finding applications in many areas[1–3]. There are many superhydrophobic surfaces in nature, such as plant leave surfaces[4,5], petal surfaces[6], water strider leg surfaces[7], insect wing surfaces[8,9], *etc*. Materials with superhydrophobic surface are in extreme demanded due to potential applications in anti-corrosion, anti-icing, liquid-repellent textiles, oil/water separation, nanoparticles assembly, microfluidic devices, printing techniques, optical devices, high-sensitive sensors and batteries[10–17]. Superhydrophobic surfaces are usually achieved by forming hierarchical micro/nanoscale binary structures and modifying the rough surface with low surface energy materials[18,19].

In the past decade, considering the significant potential of such surfaces in a number of scientific and industrial applications, researchers have made great efforts to fabricate biomimetic superhydrophobic surfaces. Up to date, many preparation methods, including template imprinting[20], plasma treatment[21], electrochemical processing[22], lithography[23], sol-gel processing[24,25], chemical vapour deposition[26,27], electrospinning[28,29], and phase separation[30,31], have been reported. However, most of the reported methods to fabricate superhydrophobic surfaces are either relatively complicated in operation or fairly expensive, which makes large scale production and application of superhydrophobic surfaces not easy to achieve.

Biomimetic hydrophobic surfaces with high or low adhesion were fabricated through a facile drop-coating method via the strategy as presented in Fig. 1. Poly(vinyl alcohol) (PVA) and SiO_2 nanoparticles were

Corresponding author: Jiang Zhou
E-mail: jiang.zhou@jlu.edu.cn

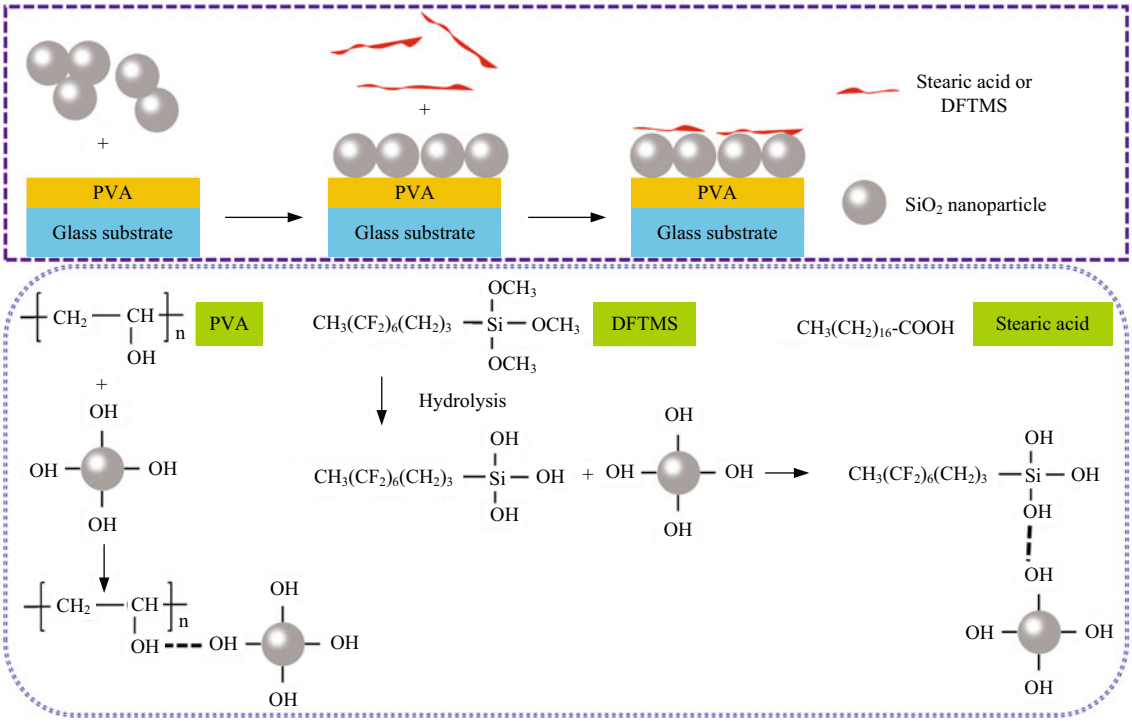

Fig. 1 Strategy for stearic acid or DFTMS modified PVA/ SiO_2 coating on glass substrate.

used to fabricate rough surfaces which showed hydrophilicity. Hydrophobicity of the prepared PVA/SiO_2 nanoparticles surfaces was achieved by modifying the surfaces with stearic acid or dodecafluoroheptyl-propyl-trimethoxysilane (DFTMS). Scanning Electron Microscope (SEM) and Atomic Force Microscope (AFM) were used to observe the morphology and topographies of the PVA/SiO_2 nanoparticle coating surfaces. Fourier Transform Infrared (FT-IR) was used to analyze the reactions between PVA and SiO_2 nanoparticles, stearic acid and SiO_2 nanoparticles, as well as DFTMS and SiO_2 nanoparticles. Water contact angles of the PVA/SiO_2 nanoparticle coating surfaces were measured to investigate the effect of surface structures (resulted from different sizes and concentrations of SiO_2 nanoparticles) and the chemical modifications on surface wettability.

2 Materials and methods

2.1 Materials

PVA with average polymerization degree of 1750 was obtained from Sinopharm Chemical Reagent Co., Ltd (Shanghai, China). Stearic acid was purchased from Tianjin Guangfu Fine Chemical Research Institute (Tianjin, China). DFTMS was purchased from XEOGIA Fluorine Silicon Chemical Co., Ltd. (Harbin, China). Absolute ethanol, tetraethyl orthosilicate and ammonium hydroxide were obtained from Beijing Chemical Works (Beijing, China). Silane coupling agents, KH-550 (NH_2-CH_2-CH_2-CH_2-Si(OC_2H_5)$_3$) and KH-560 (CH_2-CH(O)CH_2-O$(CH_2)_3$Si$(OCH_3)_3$) were supplied by Green Circle Chemical Works (Kunshan, China). SiO_2 nanoparticles with various average sizes were prepared according to Stöber's method[32] and the procedures are given in Table 1. The average size of the obtained SiO_2 nanoparticles was measured using a Malvern Zetasizer Nano-ZS90 (Malvern Instruments Ltd., UK).

2.2 Preparation of PVA/SiO_2 coatings on glass substrate

PVA solution was prepared by dissolving 15 g PVA in 500 g distilled water under stirring at 95 ˚C for 2 h. Subsequently, a cleaned glass substrate with size of 20 mm × 20 mm was coated using the PVA solution and dried in a chamber at room temperature and 33% Relative Humidity (RH). SiO_2 nanoparticles with different average sizes were dispersed into distilled water using ultrasound respectively. After continuously stirring for 30 min at room temperature, SiO_2 nanoparticle suspensions with various concentrations were obtained.

Table 1 Procedures for preparing SiO_2 nanoparticles with various average sizes

Procedure	Time (h)	Size (nm)
AE(50 mL)→Adding TEOS(1 mL)→Stiring→Adding AH(1 mL)→Stiring	6	40
AE(50 mL)→Adding TEOS(1 mL)→Stiring→Adding AH(3 mL)→Stiring	6	100
AE(50 mL)→Adding TEOS(1 mL)→Adding DW(0.3 mL)→Stiring→Adding AH(4 mL)→Stiring	6	200
AE(61.75 mL)→Adding DW(24.75 mL)→Adding AH(9mL)→Stiring→Adding TEOS(4.5 mL)→Stiring	6	400
AE(61.75 mL)→Adding DW(24.75 mL)→Adding AH(9 mL)→Stiring→Adding TEOS(4.5 mL)→Stiring	12	500
AE(100 mL)→Adding TEOS(50 mL)→Adding AH(10 mL)→Adding DW(50 mL)→Stiring	6	600
AE(100 mL)→Adding TEOS(50 mL)→Adding AH(10 mL)→Adding DW(30 mL)→Stiring	6	800

* AE (absolute ethanol); TEOS (tetraethyl orthosilicate); DW (distilled water); AH (ammonium hydroxide).

Then, 0.5 mL of the SiO_2 nanoparticle suspensions was dropped on the PVA coated glass substrate and dried at room temperature and 33% RH for 12 h.

2.3 Modification of the PVA/SiO_2 coatings via stearic acid or DFTMS

Stearic acid solution (0.01 mol·L^{-1}) was prepared by dissolving 28.4 mg stearic acid in 10 mL absolute ethanol and stirring for 30 min. DFTMS solution was obtained by mixing 1 mL DFTMS and 25 mL absolute ethanol under continuously stirring for 2 min and then adding 1 mL distilled water and stirring for 2 h at room temperature. The PVA/SiO_2 nanoparticle coating surfaces were modified by dropping the stearic acid solution or the DFTMS solution on the surfaces and drying at room temperature and 33% RH for 12 h.

2.4 Characterizations

Morphologies of SiO_2 nanoparticles, PVA/SiO_2 nanoparticle coating surfaces and stearic acid or DFTMS modified PVA/SiO_2 ones were observed using a Zeiss EVO 18 SEM (Zeiss, MERLIN Compact, Germany). The specimens were sputter-coated with gold before the observation. AFM (Dimension Icon microscope, Bruker) equipped with a Nanoscope V controller images was used to examine topographies of the coating surfaces. FT-IR spectra were recorded at resolution of 4 cm^{-1} and 32 scans using a FT-IR spectrometer (IR Affinity-1 SHIMADZU, Japan) to investigate the interactions between PVA and SiO_2 nanoparticles, stearic acid and SiO_2 nanoparticles as well as DFTMS and SiO_2 nanoparticles. The FT-IR specimens were prepared by scraping an amount of the coating from the glass substrate surface and grinding it with KBr and then pressing it into a disc. Measurements of static contact angle and dynamic sliding angle were conducted by sessile drop method at ambient temperature with 2 μL water droplets using a contact angle meter equipped with a tilting table (JC2000A, POWEREACH, China). After the static contact angle was measured, the table was tilted and the subsequent measurement of sliding angle at the same position was carried out. The tests were conducted on three different locations of each specimen, and average value was reported.

3 Results and discussions

3.1 Distributions of SiO_2 nanoparticles on silicon wafer surface

Suspensions containing SiO_2 nanoparticles of 400 nm but with different concentrations were dropped on silicon wafers. The distributions of the SiO_2 nanoparticles are shown in Figs. 2a – 2c. It can be seen that, the SiO_2 nanoparticles distribute optionally with monolayer and some of the SiO_2 nanoparticles aggregates. When the concentration of SiO_2 nanoparticle suspension increases from 1 g / 500 mL to 1 g / 125 mL, more and more SiO_2 nanoparticles aggregate and the interspaces among the SiO_2 nanoparticle aggregates become smaller. Fig. 2d presents AFM image of the surface prepared by dropping SiO_2 nanoparticle (500 nm) suspension with concentration of 1 g / 250 mL on silicon wafer. It is indicated that when the size of the SiO_2 nanoparticles is 500 nm, the suspension with concentration of 1 g / 250 mL can give rise to a close and uniform distribution of the SiO_2 nanoparticles.

3.2 Morphology and wettability of PVA/SiO_2 coating surfaces

Fig. 3 shows the accumulations of the SiO_2 nanoparticles on PVA coating surface when dropping the suspensions (containing SiO_2 nanoparticles with various average sizes) with concentration of 1 g / 50 mL. The

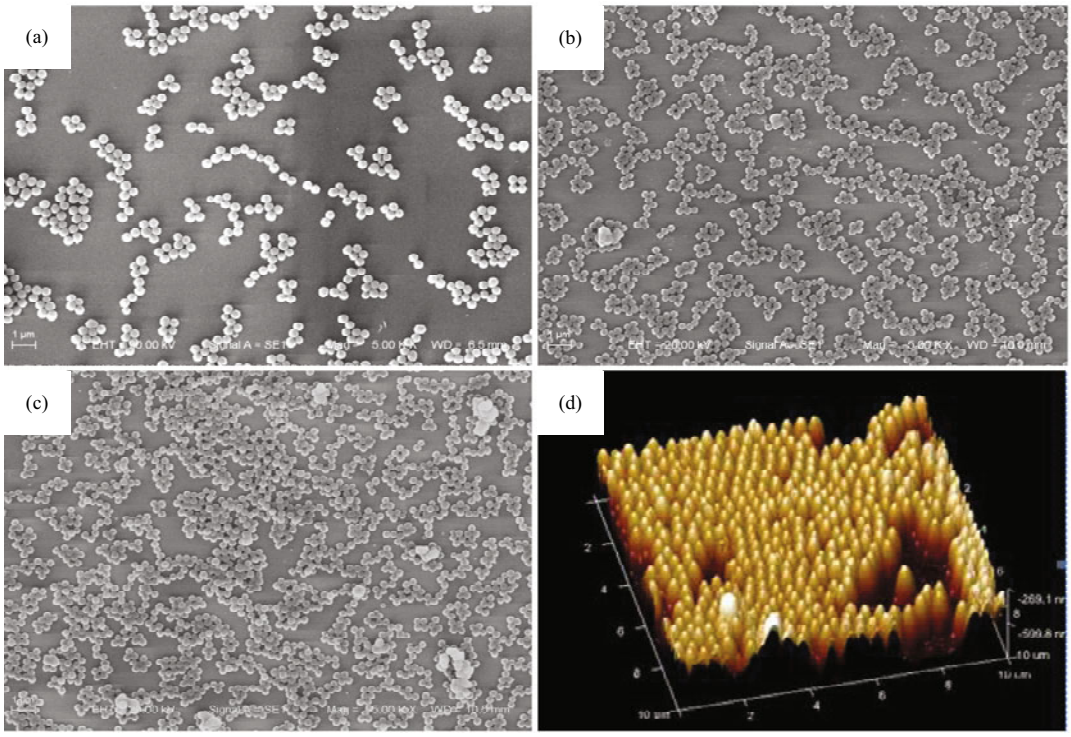

Fig. 2 Distributions of SiO_2 nanoparticles (400 nm) on silicon wafer obtained by dropping the SiO_2 nanoparticle suspensions with concentration of 1 g / 500 mL (a), 1 g / 250 mL (b) and 1 g / 125 mL (c), and AFM image of the surface prepared by dropping the SiO_2 nanoparticles (500 nm) suspension of 1 g / 250 mL on silicon wafer.

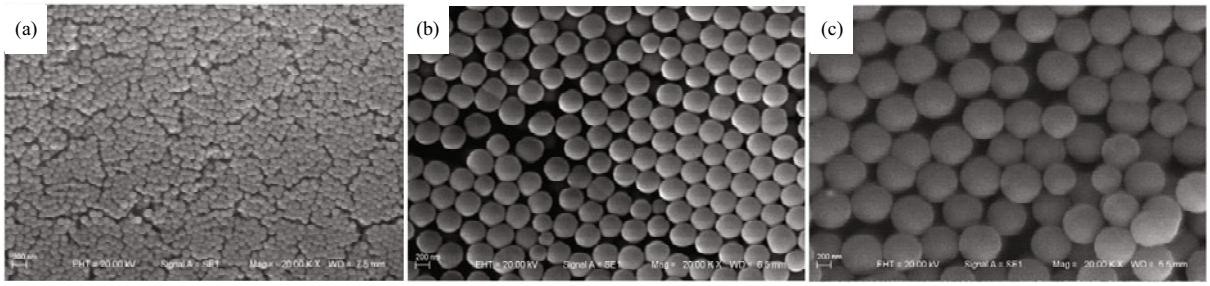

Fig. 3 SEM images of PVA/SiO_2 coating surfaces prepared by 1 g / 50 mL SiO_2 nanoparticle suspension with the SiO_2 nanoparticle size of 100 nm (a), 400 nm (b) and 600 nm (c).

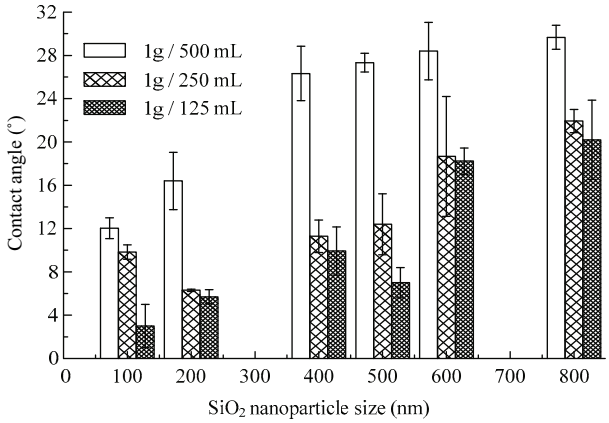

Fig. 4 Effects of SiO_2 nanoparticles size and concentration of SiO_2 nanoparticle suspension on water contact angle of the PVA/SiO_2 coating surfaces.

observations suggest that the roughness of the PVA/SiO_2 coating surfaces can be regulated by changing the size of the SiO_2 nanoparticles and the concentration of the SiO_2 nanoparticle suspensions.

Fig. 4 shows the effects of SiO_2 nanoparticle size and concentration of SiO_2 nanoparticle suspension on water contact angle of the PVA/SiO_2 coating surfaces. It can be seen that, for a given size of SiO_2 nanoparticles, the water contact angle decreases with the increase in concentration of SiO_2 nanoparticle suspension, and for a fixed concentration of SiO_2 nanoparticle suspension, the water contact angle increases with the size of SiO_2 nanoparticles except the 200 nm nanoparticles at

1 g / 250 mL and the 500 nm nanoparticles at 1 g / 125 mL. The water contact angle of the PVA/SiO_2 coating surfaces decreases from 29° to 3° when the size of SiO_2 nanoparticles decreases from 800 nm to 100 nm and the concentration of SiO_2 nanoparticle suspension increases from 1 g / 500 mL to 1 g / 125 mL, which indicates the change of surface wettability of the PVA/SiO_2 coating surfaces from hydrophilic to superhydrophilic. According to the Wenzle theoretical model, a hydrophilic surface will be more hydrophilic when the surface roughness is increased. The data in Fig. 4 suggests that the roughness of PVA/SiO_2 coating surface increases with the concentration of SiO_2 nanoparticle suspension. This is understandable, because when SiO_2 nanoparticle suspension with higher concentration was used, the extent of the SiO_2 nanoparticle aggregation on the coating surface increases, which leads to a higher surface roughness.

3.3 Morphology and wettability of the stearic acid or DFTMS modified PVA/SiO_2 nanoparticle coating surfaces

Fig. 5 shows morphologies of stearic acid and DFTMS modified PVA/SiO_2 nanoparticle (600 nm) coating surface. It can be seen that stearic acid fills the gaps among the SiO_2 nanoparticles and forms a thin film over the SiO_2 nanoparticles (Fig. 5a), which partially changes the micro structure built by the SiO_2 nanoparticles. While for the DFTMS modified one, most of the individual SiO_2 nanoparticles are coated by DFTMS and the surface structure is not changed (Fig. 5b).

In order to investigate the interactions between PVA and SiO_2, SiO_2 and stearic acid, as well as SiO_2 and DFTMS, FT-IR analysis was carried out. Fig. 6 shows the corresponding FT-IR spectra. The peaks around 3334 cm^{-1} and 1092 cm^{-1} in the spectrum of PVA (Fig. 6a) were attributed to the stretching of O-H and C-O, respectively[33]. In the spectrum of PVA/SiO_2 (Fig. 6c), the peak at 3334 cm^{-1} shifts to a lower wavenumber of 3310 cm^{-1}, and there is also a shift, from 1092 cm^{-1} to 1107 cm^{-1}, for the peak of C-O stretching. These observation results indicate that hydrogen bonds may form between the hydroxyl groups of PVA and SiO_2 nanoparticles. Figs. 6d and 6e show the FT-IR spectra of the stearic acid modified PVA/SiO_2 coating and the DFTMS modified PVA/SiO_2 coating, respectively. The absorption bands at 2919 cm^{-1} and 2851 cm^{-1} could be ascribable to the CH_3 asymmetric and CH_2 symmetric stretching vibration, and the peak of 1718 cm^{-1} in

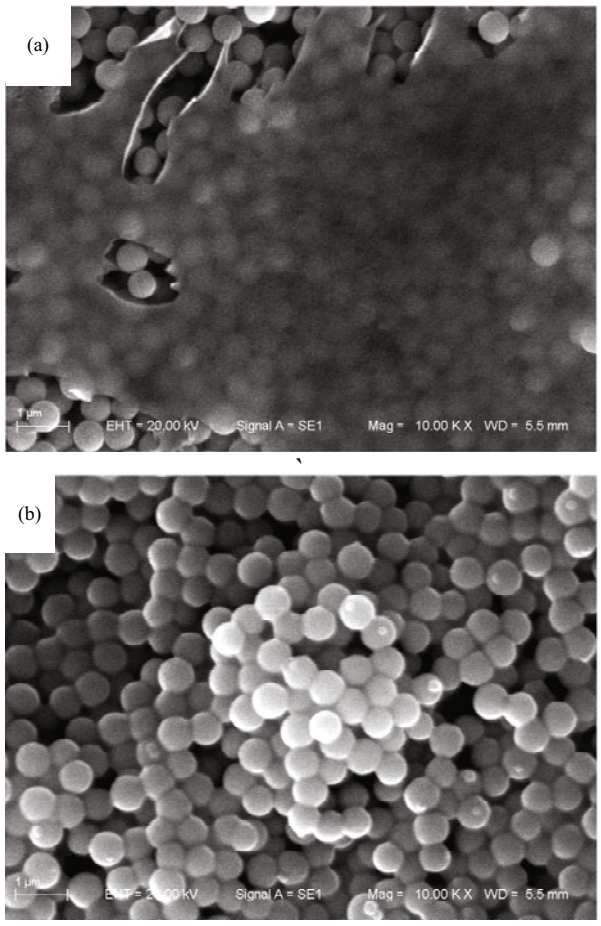

Fig. 5 SEM images of stearic acid modified PVA/SiO_2 (600 nm) coating surface with the suspension concentration of 1 g / 125 mL (a) and DFTMS modified PVA/SiO_2 (600 nm) coating surface with the suspension concentration of 1 g / 250 mL (b).

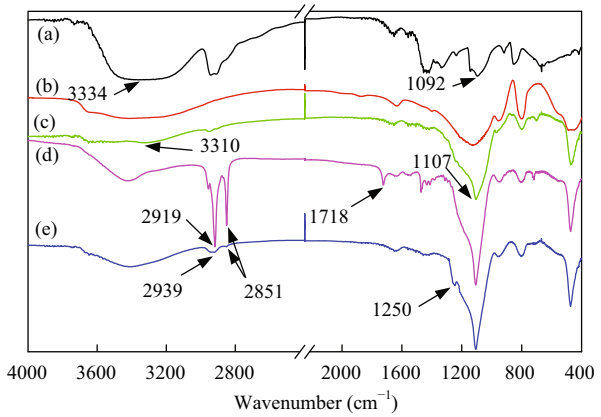

Fig. 6 FT-IR spectra of PVA (a), SiO_2 nanoparticles (b), PVA/SiO_2 coating (c), stearic acid modified PVA/SiO_2 coating (d) and DFTMS modified PVA/SiO_2 coating (e).

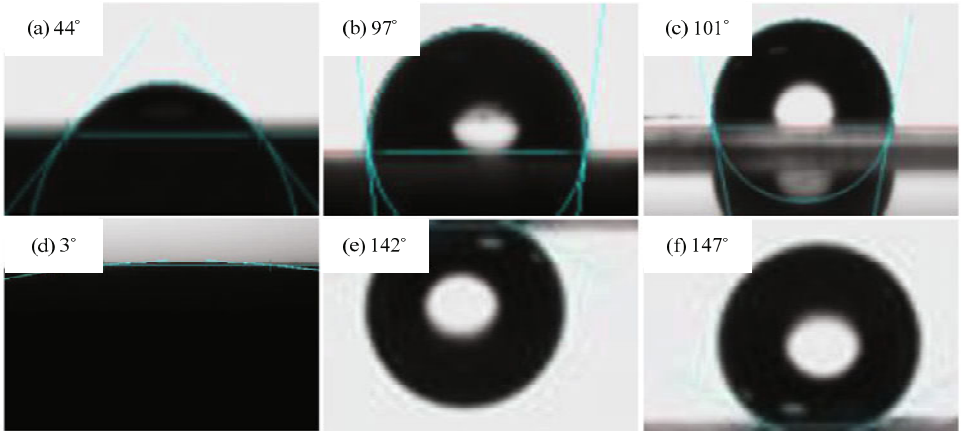

Fig. 7 Images of water droplets on the coating surface of PVA (a), stearic acid modified PVA (b), DFTMS modified PVA (c), PVA/SiO_2 (100 nm, 1 g / 125 mL) (d), stearic acid modified PVA/SiO_2 (200 nm, 1 g / 250 mL) (e), and DFTMS modified PVA/SiO_2 (100 nm, 1 g / 250 mL) (f) as well as the corresponding contact angles.

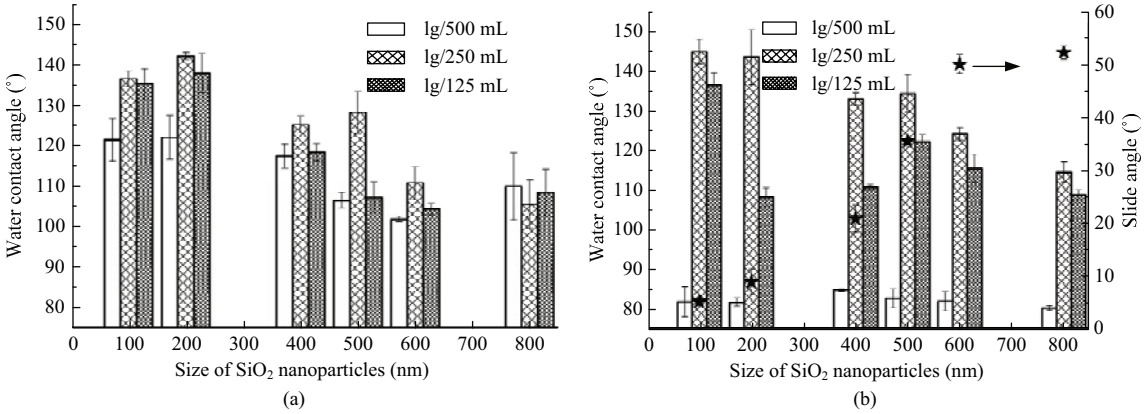

Fig. 8 Water contact angles of stearic acid modified PVA/SiO_2 coatings (a) and water contact angles and slide angles of DFTMS modified PVA/SiO_2 coatings (b).

Fig. 6d was attributable to the COO- of stearic acid[34]. While the absorption band at 1250 cm^{-1} in Fig. 6e was due to the stretching vibration of CF_2 groups[35]. Although the results of FT-IR do not provide any evidences that the interactions between SiO_2 nanoparticles and stearic acid or SiO_2 nanoparticles and DFTMS occurred, they confirm that the chemical composition of the surface was changed after the modifications.

Fig. 7 shows images of water droplets on the surfaces of PVA coating, PVA/SiO_2 coating and stearic acid or DFTMS modified ones as well as the corresponding contact angles. The water contact angle of the PVA coating is about 44°, demonstrating the hydrophilic property of this substrate. The water contact angles of the stearic acid modified PVA coating and the DFTMS modified PVA coating are 97° and 101°, respectively. Compared with that of the PVA coating surface, the water contact angle of the PVA/SiO_2 coating surface decreases significantly. The lowest water contact angle of the PVA/SiO_2 nanoparticle (100 nm, 1 g / 125 mL) coating surface is only 3°, suggesting a superhydrophilic property. However, after modification with stearic acid or DFTMS, the water contact angles of the PVA/SiO_2 coating surfaces could be up to 142° with high adhesion and 147° with low adhesion as shown in Figs. 7e and 7f. Since DFTMS has CH_2, CH_3 and CF_2 groups, while stearic acid only has CH_2 and CH_3 groups, therefore, the modification with DFTMS can reduce the free energy of the PVA/SiO_2 coating surface more effectively.

Fig. 8a shows the water contact angles of the stearic acid modified PVA/SiO_2 coating surfaces with different suspension concentrations and SiO_2 nanoparticle sizes.

It can be seen that when the size of the SiO_2 nanoparticles is smaller than or equal to 600 nm, the water contact angles of the stearic acid modified coating surfaces with suspension concentration of 1 g / 250 mL are higher than those with suspension concentrations of 1 g / 125 mL and 1 g / 500 mL. However, when the size of SiO_2 nanoparticles is 800 nm, the effect of the concentration of SiO_2 nanoparticle suspension on water contact angles of the surfaces is not significant.

Fig. 8b shows the water contact angles of the DFTMS modified PVA/SiO_2 coating surfaces with different suspension concentrations and SiO_2 nanoparticle sizes. Water contact angles of the DFTMS modified PVA/SiO_2 coating surfaces increase significantly compared with those of the unmodified PVA/SiO_2 coating surfaces shown in Fig. 4 and the surfaces exhibit hydrophobic property. It is noted that the water contact angles of the DFTMS modified PVA/SiO_2 coating surfaces range from 80˚ to 85˚ when the concentration of SiO_2 nanoparticle suspension is 1 g / 500 mL, and the effect of the DFTMS modification is not significant. This may be because the low concentration of SiO_2 nanoparticle suspension (1 g / 500 mL) gives rise to large interspaces among the SiO_2 nanoparticles and low surface roughness as shown in Fig. 2a. When the concentration of SiO_2 nanoparticle suspension is 1 g / 250 mL, the water contact angles of the DFTMS modified PVA/SiO_2 coating surfaces range from 115˚ to 147˚ suggesting that the surfaces become hydrophobic. The data in Fig. 8b also shows that, for a given size of SiO_2 nanoparticles, the water contact angles of the DFTMS modified PVA/SiO_2 coating surfaces with 1 g / 250 mL suspension concentration are larger than that with 1 g / 125 mL suspension concentration, and the water contact angles decrease with the increase in the size of SiO_2 nanoparticles except the 500 nm when the suspension concentration is 1 g / 250 mL. These results may be because that the increase in the concentration of SiO_2 nanoparticle suspension or the size of the SiO_2 nanoparticles causes a reduction in roughness of the coating surface. As for a hydrophobic surface, the higher the surface roughness, the stronger the hydrophobicity.

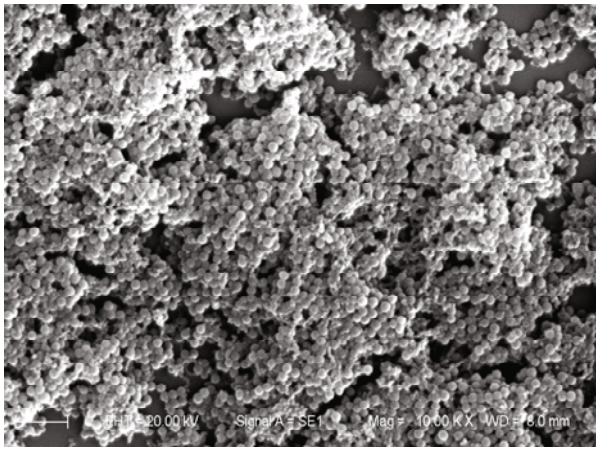

Fig. 9 SEM image of the surface structure obtained by dropping the mixture of the suspensions containing 40 nm SiO_2 nanoparticles and 200 nm SiO_2 nanoparticles on silicon wafer.

It is known that if a hydrophobic surface has a slide angle smaller than 10˚, the surface will show low adhesion, which means that water droplets can easily roll away from the surface. Fig. 8b shows that the slide angle of the DFTMS modified PVA/SiO_2 coating surface prepared with 1 g / 250 mL SiO_2 nanoparticle suspension decreases with the reduction of the SiO_2 nanoparticle size, and reaches to 5˚ when the size of SiO_2 nanoparticles is 100 nm. These results indicate that the DFTMS modified PVA/SiO_2 coating surfaces could have hydrophobicity and low adhesion characteristics.

Wettability of the DFTMS modified PVA/SiO_2 nanoparticle (40 nm plus 200 nm) coating surface was also investigated. 0.3 mL of KH550 and KH560 were added into 50 mL of the suspensions containing 40 nm SiO_2 nanoparticles and 200 nm SiO_2 nanoparticles, respectively, and stirred for 3 h. Then the two suspensions were mixed by stirring at 60 ˚C for 4 h. Fig. 9 shows the surface structure obtained by dropping the prepared mixture of the two suspensions on silicon wafer. Compared with the surfaces fabricated with single size of SiO_2 nanoparticles (Fig. 3), the surface structure prepared with mixed sizes of SiO_2 nanoparticles (40 nm plus 200 nm) is much rougher. The water contact angle of the DFTMS modified PVA/SiO_2 nanoparticle (40 nm plus 200 nm) coating surface is up to 155˚ and the slide angle is only 5˚, indicating the coating surface has superhydrophobicity and low adhesion characteristics.

To understand the hydrophobicity with low and high adhesion behavior of the surfaces, the mechanism affecting the adhesion is analyzed. Fig. 10 shows a schematic diagram of a water droplet on solid surface. If the interface is the Cassie impregnating wetting state (Fig. 10b), the surface will show high adhesion behavior to a water droplet like rose petal, due to the van der

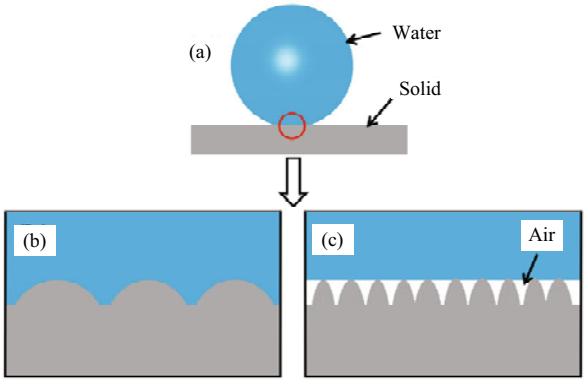

Fig. 10 Schematic diagrams of a water droplet on solid surface (a), the Cassie impregnating wetting state (b) and the Cassie water/air/solid three-phase state (c).

Waals force produced by large liquid−solid contact area between the water droplet and the substrate[36,37]. If the interface is the Cassie water/air/solid three-phase state (Fig. 10c), large amount of air are trapped in the nano-scale structure, and the surface will show superhydrophobicity and low adhesion like lotus leaf[38]. In this work, both the stearic acid and DFTMS modified PVA/SiO_2 coating surfaces have hydrophobicity but show different adhesion to water. The reason could be the difference in the micro/nano surface structure. Fig. 5a shows that stearic acid partially changes the micro structure built by the SiO_2 nanoparticles, and the modified coating surface shows hydrophobicity with high adhesion (Fig. 7e). However, DFTMS modified PVA/SiO_2 coating surface shows hydrophobicity with low adhesion (Fig. 8b) because that the surface structure is not changed (Fig. 5b).

4 Conclusion

Biomimetic hydrophobic PVA/SiO_2 coating surface with high adhesion and superhydrophobic PVA/SiO_2 coating surface with low adhesion were successfully prepared by using SiO_2 nanoparticles to fabricate surface roughness and stearic acid or DFTMS as low surface energy materials to modify the obtained surfaces. The water contact angles of the PVA/SiO_2 coating surfaces increase with the size of SiO_2 nanoparticles and the hydrophilic property is enhanced by increasing concentration of SiO_2 nanoparticle suspensions. The water contact angle of the obtained superhydrophilic coating surface could reach to 3˚. The water contact angle of the PVA/SiO_2 nanoparticle (200 nm, 1 g / 250 mL) coating surface modified by stearic acid is 142˚ with high adhesion. The PVA/SiO_2 nanoparticle (40 nm plus 200 nm) coating surface modified with DFTMS shows superhydrophobic characteristic with water contact angle of 155˚ and low adhesion with slide angle of 5˚. The hydrophilicity of the PVA/SiO_2 coating surfaces and hydrophobicity of the stearic acid or DFTMS modified PVA/SiO_2 coating surfaces could be regulated by controlling the size of SiO_2 nanoparticles and concentration of SiO_2 nanoparticle suspensions. The present work provides a facile method to change the wettability of PVA/SiO_2 coating surfaces and broaden applications of PVA/SiO_2 coatings as superhydrophilic surface or superhydrophobic surface with low or high adhesion.

Acknowledgment

This work is supported by the National Natural Science Foundation of China (51273083 and 51405188) and China Postdoctoral Science Foundation (2015T80307).

References

[1] Bravo J, Zhai L, Wu Z Z, Cohen R E, Rubner M F. Transparent superhydrophobic films based on silica nanoparticles. *Langmuir*, 2007, **23**, 7293–7298.

[2] Zhang X, Feng S, Jia N, Jiang Y, Wang Z. Superhydrophobic surfaces: From structural control to functional application. *Journal of Materials Chemistry*, 2008, **18**, 621–633.

[3] Fujishima A, Zhang X, Tryk D A. TiO_2 photocatalysis and related surface phenomena. *Surface Science Reports*, 2008, **63**, 515–582.

[4] Koch K, Bhushan B, Barthlott W. Diversity of structure, morphology and wetting of plant surfaces. *Soft Materials*, 2008, **4**, 1943–1963.

[5] Koch K, Bhushan B, Barthlott W. Multifunctional surface structures of plants: An inspiration for biomimetics. *Progress in Materials Science*, 2009, **54**, 137–178.

[6] Feng L, Zhang Y, Xi J, Zhu Y, Wang N, Xia F, Jiang L. Petal effect: A superhydrophobic state with high adhesive force. *Langmuir*, 2008, **24**, 4114–4119.

[7] Gao X, Jiang L. Water-repellent legs of water striders. *Nature*, 2004, **432**, 36.

[8] Byun D, Hong J, Saputra, Ko J H, Lee Y J, Park H C, Byun B-K, Lukes J R. Wetting characteristics of insect wing surfaces. *Journal of Bionic Engineering*, 2009, **6**, 63–70.

[9] Fang Y, Sun G, Cong Q, Chen G, Ren L. Effects of methanol on wettability of the non-smooth surface on butterfly wing.

Journal of Bionic Engineering, 2008, **5**, 127–133.

[10] Darmanin T, Guittard F. Recent advances in the potential applications of bioinspired superhydrophobic materials. *Journal of Materials Chemistry A*, 2014, **2**, 16319–16359.

[11] Li H, Wang J, Yang L, Song Y. Superoleophilic and superhydrophobic inverse opals for oil sensors. *Advanced Functional Materials*, 2008, **18**, 3258–3264.

[12] Wang J, Zhang Y, Wang S, Song Y, Jiang L. Bioinspired colloidal photonic crystals with controllable wettability. *Accounts of Chemical Research*, 2011, **44**, 405–415.

[13] Shen W, Li M, Ye C, Jiang L, Song Y. Direct-writing colloidal photonic crystal microfluidic chips by inkjet printing for label-free protein detection. *Lab on a Chip*, 2012, **12**, 3089–3095.

[14] Hou J, Zhang H, Yang Q, Li M, Song Y, Jiang L. Bio-inspired photonic-crystal microchip for fluorescent ultratrace detection. *Angewandte Chemie-International Edition*, 2014, **53**, 5791–5795.

[15] Tian D, Song Y, Jiang L. Patterning of controllable surface wettability for printing techniques. *Chemical Society Reviews*, 2013, **42**, 5184–5209.

[16] Huang Y, Zhou J, Su B, Shi L, Wang J, Chen S, Wang L, Zi J, Song Y, Jiang L. Colloidal photonic crystals with narrow stopbands assembled from low-adhesive superhydrophobic substrates. *Journal of the American Chemical Society*, 2012, **134**, 17053–17058.

[17] Xue Z, Wang S, Lin L, Chen L, Liu M, Feng L, Jiang L. A novel superhydrophilic and underwater superoleophobic hydrogel-coated mesh for oil/water separation. *Advanced Materials*, 2011, **23**, 4270-4273.

[18] Chen H, Zhang X, Zhang P, Zhang Z. Facile approach in fabricating superhydrophobic SiO_2/polymer nanocomposite coating. *Applied Surface Science*, 2012, **261**, 628–632.

[19] Li H, Yu S, Han X, Zhang S, Zhao Y. A simple method for fabrication of bionic superhydrophobic zinc coating with crater-like structures on steel substrate. *Journal of Bionic Engineering*, 2016, **13**, 622–630.

[20] Lee Y, Park S-H, Kim K-B, Lee J-K. Fabrication of hierarchical structures on a polymer surface to mimic natural superhydrophobic surfaces. *Advanced Materials*, 2007, **19**, 2330–2335.

[21] Fernández-Blázquez J P, Fell D, Bonaccurso E, del Campo A. Superhydrophilic and superhydrophobic nanostructured surfaces via plasma treatment. *Journal of Colloid and Interface Science*, 2011, **357**, 234–238.

[22] Darmanin T, de Givenchy E T, Amigoni S, Guittard F. Superhydrophobic surfaces by electrochemical processes. *Advanced Materials*, 2013, **25**, 1378–1394.

[23] Sung Y H, Kim Y D, Choi H-J, Shin R, Kang S, Lee H. Fabrication of superhydrophobic surfaces with nano-in-micro structures using UV-nanoimprint lithography and thermal shrinkage films. *Applied Surface Science*, 2015, **349**, 169–173.

[24] Rao A V, Latthe S S, Nadargi D Y, Hirashima H, Ganesan V. Preparation of MTMS based transparent superhydrophobic silica films by sol–gel method. *Journal of Colloid and Interface Science*, 2009, **332**, 484–490.

[25] Manca M, Cannavale A, De Marco L, Aricò A S, Cingolani R, Gigli G. Durable superhydrophobic and antireflective surfaces by trimethylsilanized silica nanoparticles-based sol–gel processing. *Langmuir*, 2009, **25**, 6357–6362.

[26] Crick C R, Ismail S, Pratten J, Parkin I P. An investigation into bacterial attachment to an elastomeric superhydrophobic surface prepared via aerosol assisted deposition. *Thin Solid Films*, 2011, **519**, 3722–3727.

[27] Crick C R, Gibbins J A, Parkin I P. Superhydrophobic polymer-coated copper-mesh; membranes for highly efficient oil–water separation. *Journal of Materials Chemistry A*, 2013, **1**, 5943–5948.

[28] Nuraje N, Khan W S, Lei Y, Ceylan M, Asmatulu R. Superhydrophobic electrospun nanofibers. *Journal of Materials Chemistry A*, 2013, **1**, 1929–1946.

[29] Yoshida H, Klee D, Möller M, Akashi M. Creation of superhydrophobic electrospun nonwovens fabricated from naturally occurring poly (amino acid) derivatives. *Advanced Functional Materials*, 2014, **24**, 6359–6364.

[30] Wu Z, Wang H, Tian X, Xue M, Ding X, Ye X, Cui Z. Surface and mechanical properties of hydrophobic silica contained hybrid films of waterborne polyurethane and fluorinated polymethacrylate. *Polymer*, 2014, **55**, 187–194.

[31] Kato S, Sato A. Micro/nanotextured polymer coatings fabricated by UV curing-induced phase separation: Creation of superhydrophobic surfaces. *Journal of Materials Chemistry*, 2012, **22**, 8613–8621.

[32] Stöber W, Frank A, Bohn E. Controlled growth of monodisperse silica spheres in the micron size range. *Journal of Colloid and Interface Science*, 1968, **26**, 62–69.

[33] Şanlı O, Karaca I, Işıklan N. Preparation, characterization, and salicylic acid release behavior of chitosan/poly(vinyl alcohol) blend microspheres. *Journal of Applied Polymer Science*, 2009, **111**, 2731–2740.

[34] Musto P, Larobina D, Cotugno S, Straffi P, Florio G D, Mensitieri G. Confocal Raman imaging, FTIR spectroscopy and kinetic modelling of the zinc oxide/stearic acid reaction in a vulcanizing rubber. *Polymer*, 2013, **54**, 685–693.

[35] Qing Y, Zheng Y, Hu C, Wang Y, He Y, Gong Y, Mo Q.

Facile approach in fabricating superhydrophobic ZnO/polystyrene nanocomposite coating. *Applied Surface Science*, 2013, **285**, 583–587.

[36] Liu Y, Liu J, Li S, Liu J, Han Z, Ren L. Biomimetic superhydrophobic surface of high adhesion fabricated with micronano binary structure on aluminum alloy. *ACS Applied Materials & Interfaces*, 2013, **18**, 8907–8914.

[37] Zhang Y-L, Chen Q-D, Jin Z, Kim E, Sun H-B. Biomimetic graphene films and their properties. *Nanoscale*, 2012, **4**, 4858–4869.

[38] Chen P, Chen L, Han D, Zhai J, Zheng Y, Jiang L. Wetting behavior at micro-/nanoscales: Direct imaging of a microscopic water/air/solid three-phase interface. *Small*, 2009, **5**, 908–912.